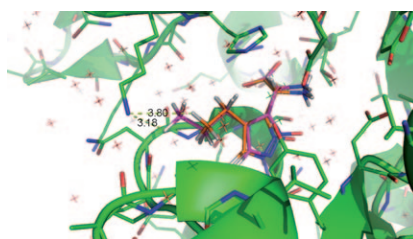


Subunit selectivity at NMDA receptors: Subunit-selective ligands for the glutamate receptors remain an area of interest, since glutamate is the major excitatory neurotransmitter in the brain and involved in a number of diseased states in the central nervous system. Few selective ligands are known, especially among the NMDA receptor class. Development of these ligands seems to be a difficult task because of the conserved region in the binding site of the NMDA receptor subunits. A scaffold developed by our group has shown potential to differentiate among the NMDA receptor subunits.



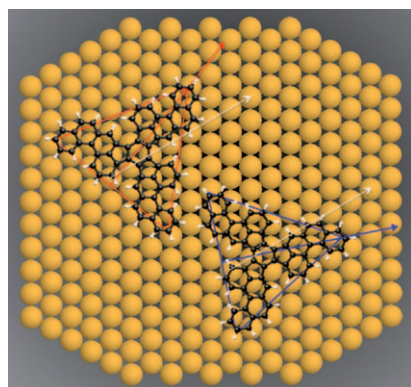
Receptors

*R. Risgaard, K. B. Hansen,
R. P. Clausen** 13910–13918

Partial Agonists and Subunit Selectivity at NMDA Receptors

COMMUNICATIONS

Surface control: Vacuum deposition of a planarized PAH ($C_{60}H_{30}$) on a Pt-(111) surface induces chirality caused by the different landing side of the molecule, as shown by in situ STM images. The surface determines the landing side of individual molecules, which present different structural geometries that are shifted by about 35° (see figure). Large-scale calculations explain the atomistic mechanism of the process.



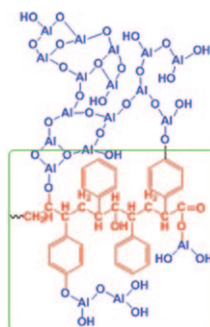
Surface–Molecule Interactions

*G. Otero, G. Biddau, T. Ozaki,
B. Gómez-Lor, J. Méndez, R. Pérez,*
J. A. Martín-Gago** 13920–13924

Spontaneous Discrimination of Polycyclic Aromatic Hydrocarbon (PAH) Enantiomers on a Metal Surface



One layer at a time: A proposed growth mechanism of Al_2O_3 atomic layer deposition on a polystyrene surface is presented. The infiltration of trimethylaluminum and H_2O precursors may result in Al_2O_3 growth in the polystyrene matrix (subsurface), thus forming a hybrid interface (shown in the green box) of $C_8H_7O^-$ and $C_6H_4O_2Al^-$ ions.



Metal Oxide Films

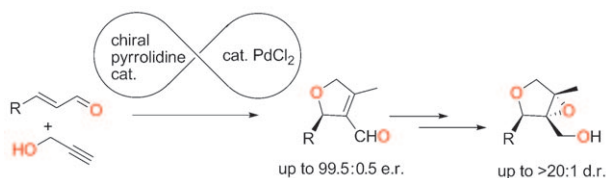
*M. Puttaswamy, K. B. Haugshøj,
L. Højslet Christensen,
P. Kingshott** 13925–13929

Molecular Mechanisms of Aluminum Oxide Thin Film Growth on Polystyrene during Atomic Layer Deposition



Asymmetric Catalysis

S. Lin, G.-L. Zhao,* L. Deiana, J. Sun,
Q. Zhang, H. Leijonmarck,
A. Córdova* 13930–13934



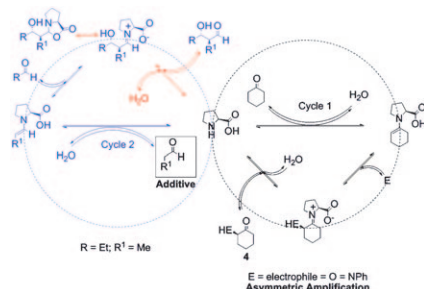
Dynamic Kinetic Asymmetric Domino Oxa-Michael/Carbocyclization by Combination of Transition-Metal and Amine Catalysis: Catalytic Enantioselective Synthesis of Dihydrofurans

Into the pot: A one-pot highly chemo- and enantioselective catalytic domino oxa-Michael/carbocyclization between α,β -unsaturated aldehydes and propargylic alcohols is presented. This

dynamic kinetic transformation requires a combination of transition-metal and amine catalysis to afford functionalized dihydrofurans in good to high yields and up to 99.5:0.5 e.r.

Asymmetric Catalysis

R. Rios, P. Schyman, H. Sundén,
G.-L. Zhao, F. Ullah, L.-J. Chen,
A. Laaksonen,
A. Córdova* 13935–13940

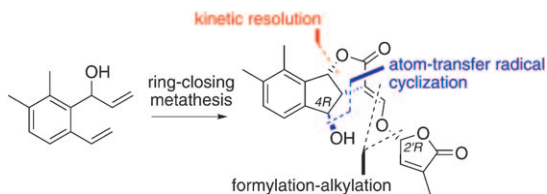


Nonlinear Effects in Asymmetric Amino Acid Catalysis by Multiple Interconnected Stereoselective Catalytic Networks

A fine line: The generation of significant positive nonlinear effects in asymmetric amino acid catalysis under homogeneous conditions, which can be explained by the model for cooperative catalytic stereoselective pathways, is reported. The addition of an achiral aldehyde generated the multiple interconnected stereoselective catalytic network.

Natural Products

V. X. Chen, F.-D. Boyer,* C. Rameau,
P. Retailleau, J.-P. Vors,
J.-M. Beau* 13941–13945



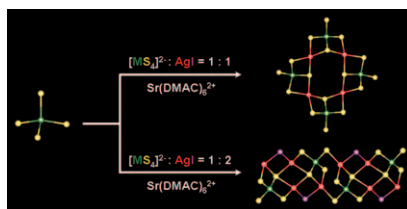
Stereochemistry, Total Synthesis, and Biological Evaluation of the New Plant Hormone Solanacol

The first total synthesis of solanacol, a member of the strigolactone family, features ring-closing metathesis, enzymatic kinetic resolution, and atom-transfer radical cyclization. This

defines the stereostructure of the natural product. The best hormonal activity is revealed by an acetylated derivative at O4 (see scheme).

Cluster Compounds

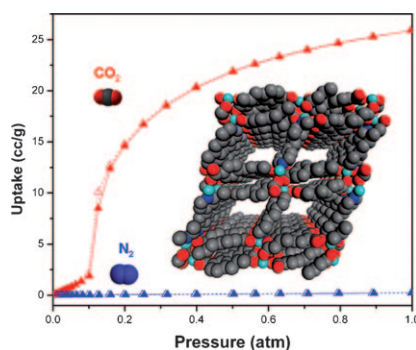
J. Zhang, S. Meng, Y. Song, H. Zhao,
J. Li, G. Qu, L. Sun,
M. G. Humphrey,*
C. Zhang* 13946–13950



Facile Syntheses and Tunable Non-Linear Optical Properties of Heterothiometallic Clusters with [MS₄Ag₂] Units (M=Mo, W)

A not-so-innocent counterion: A facile synthetic method has been successfully developed to construct two unusual discrete, octanuclear planar “open” distorted-square M/S/Ag clusters $\{[\text{Sr}(\text{DMAC})_6]_2[\text{M}_4\text{S}_{16}\text{Ag}_4]\}$ (M=Mo, W; DMAC = *N,N'*-dimethylacetamide) and a unique 1D double-chain W/S/Ag cluster $\{[\text{Sr}(\text{DMAC})_6][\text{W}_2\text{S}_8\text{Ag}_4\text{I}_2]\}_n$ (see figure). Z-scan experiments show that $\{[\text{Sr}(\text{DMAC})_6]_2[\text{Mo}_4\text{S}_{16}\text{Ag}_4]\}$ exhibits strong third-order non-linear optical properties and a large optical limiting capability.

Caught in a CO₂ trap: A highly flexible microporous metal–organic framework material exhibits a remarkable ability to capture and separate carbon dioxide from other small gases, such as N₂, H₂, CH₄, CO, and O₂, with separation ratios of 294, 190, 257, and 441 for CO₂/N₂, CO₂/H₂, CO₂/CH₄, and CO₂/CO, respectively, at 0.16 atm and 25 °C, and 768 for CO₂/O₂ at 0.2 atm and 25 °C.



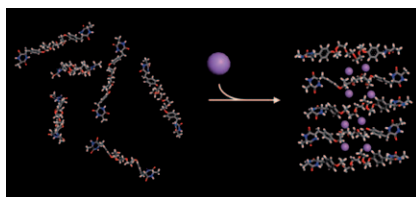
Microporous Materials

*H. Wu, R. S. Reali, D. A. Smith, M. C. Trachtenberg, J. Li** 13951–13954

Highly Selective CO₂ Capture by a Flexible Microporous Metal–Organic Framework (MMOF) Material



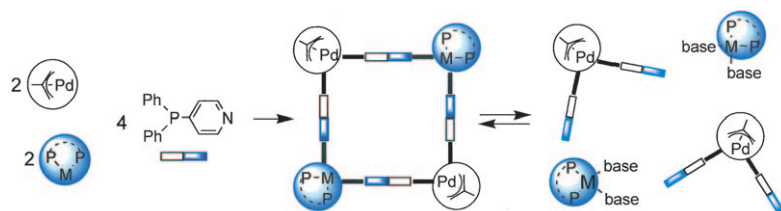
Stuck Li-ke glue: Oligo(ethylene oxide)-bridged bis(cyclodipeptides) exhibited remarkable enhancement of gelation ability by the addition of Li⁺ (see figure). By coordination of metal ions to the oligo(ethylene oxide) chain, terminal cyclodipeptides may move closer and more easily form the hydrogen-bonded-sheet structure of cyclodipeptides.



Supramolecular Gels

*J.-A. Kim, Y.-H. Jeong, W.-D. Jang** 13955–13959

Versatile Supramolecular Gelling Agents: Unusual Stabilization of Physical Gels by Lithium Ions



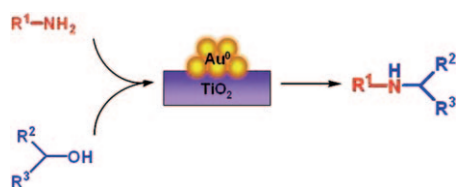
Hip to be square: Tetranuclear metalamacrocycles containing Pd–allyl and either Pd(dppp) or Pt(dppp) moieties (dppp = 1,3-bis(diphenylphosphino)propane) have been obtained from the selective combination of three differ-

ent building blocks. The study of their unusual dynamic behavior demonstrated the equilibrium between the self-assembled supramolecules and their components (see scheme).

Supramolecular Chemistry

I. Angurell, M. Ferrer, A. Gutiérrez, M. Martínez, L. Rodríguez, O. Rossell, M. Engeser* 13960–13964

Antisymbiotic Self-Assembly and Dynamic Behavior of Metallamacrocycles with Allylic Corners



Atom-efficient direct N-alkylation: An environmentally clean one-pot selective N-alkylation of amines with an equimolar amount of alcohols via a

hydrogen autotransfer pathway was achieved over a titania-supported gold catalyst system in good to excellent yields without additive (see scheme).

Heterogeneous Catalysis

L. He, X.-B. Lou, J. Ni, Y.-M. Liu, Y. Cao, H.-Y. He, K.-N. Fan* 13965–13969

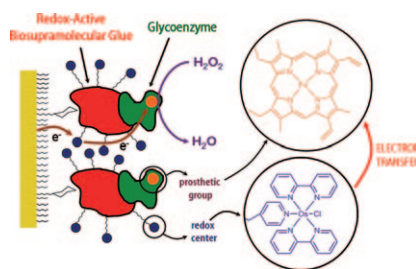
Efficient and Clean Gold-Catalyzed One-Pot Selective N-Alkylation of Amines with Alcohols



Supramolecular Assembly

D. Pallarola, N. Queraltó, W. Knoll,
O. Azzaroni,*
F. Battaglini 13970–13975

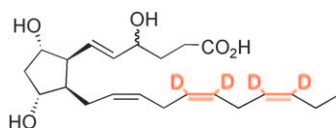
Facile Glycoenzyme Wiring to Electrode Supports by Redox-Active Biosupramolecular Glue



It has to be glue! The use of redox-active concanavalin A as a bifunctional building block enables the recognition-directed assembly of HRP layers on bioelectronic platforms and the communication of the prosthetic group of the enzyme to the electrode surface (see figure).

Retrosynthesis

C. Oger, V. Bultel-Poncé, A. Guy,
L. Balas, J.-C. Rossi, T. Durand,
J.-M. Galano* 13976–13980



Brown's P2-Ni does the job: An efficient synthesis of tetradecaterated neuroprostane (see structure) has been accomplished by using an ene-diyne stereoselective deuteration strategy.

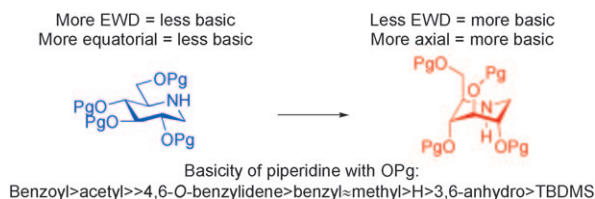
The Handy Use of Brown's P2-Ni Catalyst for a Skipped Diyne Deuteration: Application to the Synthesis of a [D₄]-Labeled F_{4t}-Neuroprostane

FULL PAPERS

Protecting Groups

M. Heuckendorff, C. M. Pedersen,*
M. Bols* 13982–13994

VIP Quantifying Electronic Effects of Common Carbohydrate Protecting Groups in a Piperidine Model System



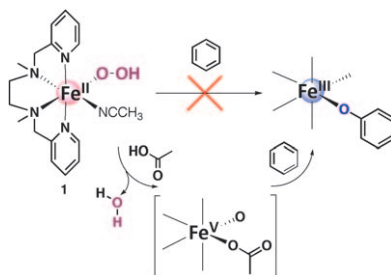
Carbohydrates at arms: How great an influence protecting groups have on the reactivity of carbohydrates has been determined. The protecting groups in a “disarmed” saccharide are more than 300 times more electron

withdrawing (EWD) than those in an “armed” saccharide and those of a “superarmed” saccharide are 300 times less EWD (see scheme, TBDMS = *tert*-butyldimethylsilyl).

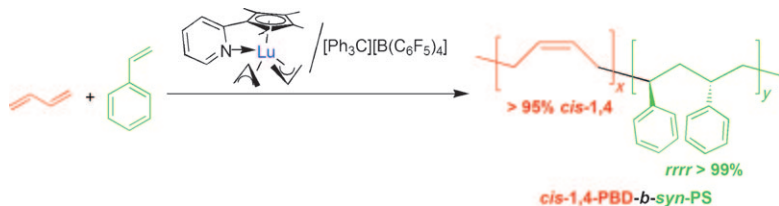
Aromatic Hydroxylation

O. V. Makhlynets,
E. V. Rybak-Akimova* . . 13995–14006

VIP Aromatic Hydroxylation at a Non-Heme Iron Center: Observed Intermediates and Insights into the Nature of the Active Species



Iron out the rough spots: [Fe(bpmen)-(CH₃CN)₂][ClO₄]₂ (**1**), an excellent catalyst for organic oxidations with hydrogen peroxide, is found to efficiently promote hydroxylation of benzene. This new reaction revealed mechanistic pathways in hydrogen peroxide activation with complex **1**. Detailed kinetic and mechanistic studies showed that Fe^{III}(OOH) produces the reactive species in the rate-limiting, acid-assisted heterolytic cleavage of the O–O bond in the iron-peroxo intermediate.



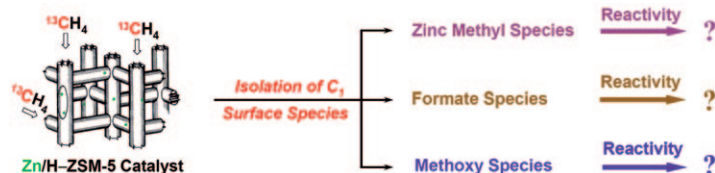
Challenge to a dual: Under the activation of $[\text{Ph}_3\text{C}][\text{B}(\text{C}_6\text{F}_5)_4]$, a pyridyl-functionalized cyclopentadienyl lutetium-bis(allyl) complex exhibited

unprecedented dual behavior for syndiotactic ($rrrr > 99\%$) styrene polymerization and *cis*-1,4-selective (99%) butadiene polymerization.

Polymerization

Z. Jian, S. Tang, D. Cui* 14007–14015

A Lutetium Allyl Complex That Bears a Pyridyl-Functionalized Cyclopentadienyl Ligand: Dual Catalysis on Highly Syndiospecific and *cis*-1,4-Selective (Co)Polymerizations of Styrene and Butadiene



Reactivity of C_1 surface species: Zinc methyl species, formate species, and methoxy species were identified as C_1 surface species formed in methane activation on the zeolite Zn/H-ZSM-5

catalyst at $T \leq 573$ K (see graphic). We successfully isolated each surface species and investigated their chemical nature on the working catalyst by solid-state NMR spectroscopy.

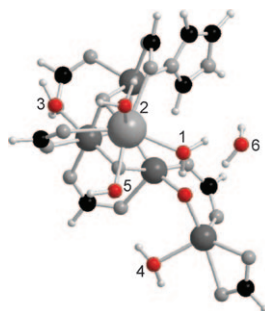
Methane Activation

J. F. Wu, W. D. Wang, J. Xu, F. Deng, W. Wang* 14016–14025

Reactivity of C_1 Surface Species Formed in Methane Activation on Zn-Modified H-ZSM-5 Zeolite



Water ways: Density functional calculations are reported on a set of three model structures of the Mn_4Ca cluster in the water-oxidizing complex of Photosystem II (see figure). The preferred hydration sites across five oxidation states and all feasible magnetic-coupling arrangements have been explored to identify the most likely substrate–water binding sites.



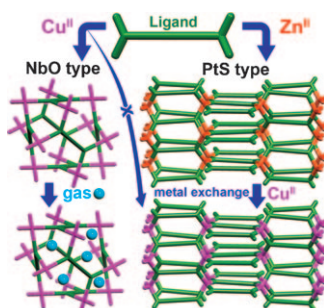
Photosystem II

S. Petrie, R. Stranger,*
R. J. Pace 14026–14042

Hydration Preferences for Mn_4Ca Cluster Models of Photosystem II: Location of Potential Substrate–Water Binding Sites



Unprecedented oxygen capacity: Synthesis of a Cu^{II} -based metal–organic framework (MOF) with NbO-type net structure that shows high adsorption capacities for N_2 , H_2 , O_2 , CO_2 , and CH_4 is reported. A similar reaction with Zn^{II} afforded a PtS-type net. Post-synthetic metal-ion exchange of a Zn^{II} MOF with Cu^{II} resulted in a Cu^{II} MOF with a PtS-type net that could not be obtained from direct synthesis (see figure).



Metal–Organic Frameworks

T. K. Prasad, D. H. Hong,
M. P. Suh* 14043–14050

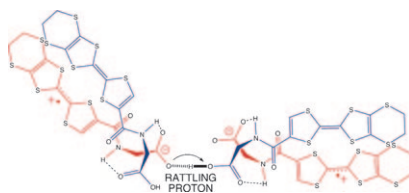
High Gas Sorption and Metal-Ion Exchange of Microporous Metal–Organic Frameworks with Incorporated Imide Groups



Organic Electronics

A. El-Ghayoury, C. Mézière,
S. Simonov, L. Zorina, M. Cobián,
E. Canadell, C. Rovira, B. Náfrádi,
B. Sipoš, L. Forró,
P. Batail* 14051–14059

 **A Neutral Zwitterionic Molecular Solid**

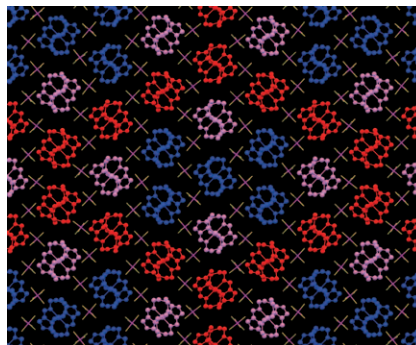


Electrostatic envelope: Two neutral chemical objects with ionizable residues, one of which is a π -conjugated zwitterion, self-assemble in a two-dimensional array (see picture). It is predicted that the carriers are probably localized, yet the system is highly conducting. Although not part of the conducting network, a rattling proton deeply impinges on the collective behavior of the holes.

Molecular Spin-States

N. Bréfuel, E. Collet,* H. Watanabe,
M. Kojima, N. Matsumoto, L. Toupet,
K. Tanaka,
J.-P. Tuchagues* 14060–14068

Nanoscale Self-Hosting of Molecular Spin-States in the Intermediate Phase of a Spin-Crossover Material

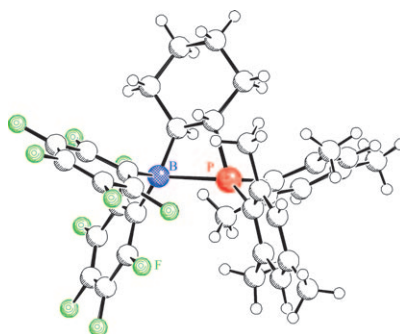


Nanoscale self-hosting of spin-state: Thermally induced spin crossover associated with symmetry breaking yields an unprecedented long-range ordering in the intermediate (INT) phase (supercell structure of 30 molecules) of a novel molecular material based on an iron complex. A remarkable lozenge pattern is produced, including 12 predominantly high-spin (HS), 8 predominantly low-spin (LS), and 10 purely LS molecular crystallographic sites (red, purple, and blue, respectively, in figure).

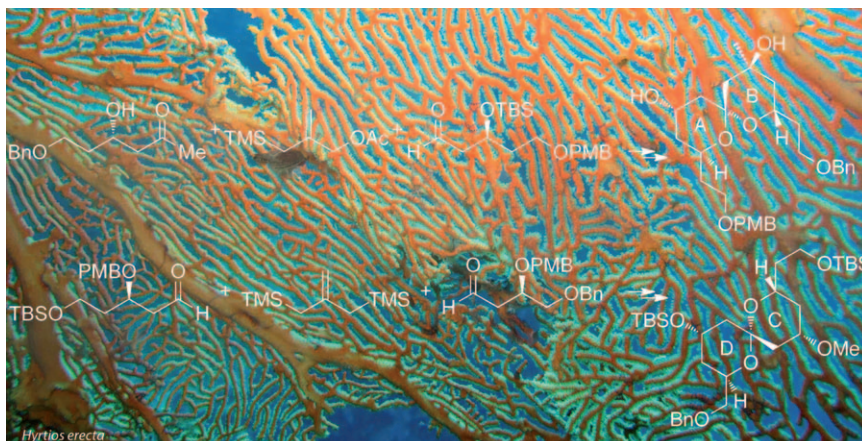
Frustrated Lewis Pairs

K. V. Axenov, C. M. Mömmling,
G. Kehr, R. Fröhlich,
G. Erker* 14069–14073

 **Structure and Dynamic Features of an Intramolecular Frustrated Lewis Pair**



The cyclohexylene-anellated frustrated Lewis pair was obtained by hydroboration of di(mesityl)cyclohexenylphosphine with $[\text{HB}(\text{C}_6\text{F}_5)_2]$. The X-ray crystal structure analysis (see picture) revealed a puckered four-membered heterocyclic core. The compound splits dihydrogen heterolytically and adds to the $\text{C}=\text{O}$ bond of phenyl isocyanate.



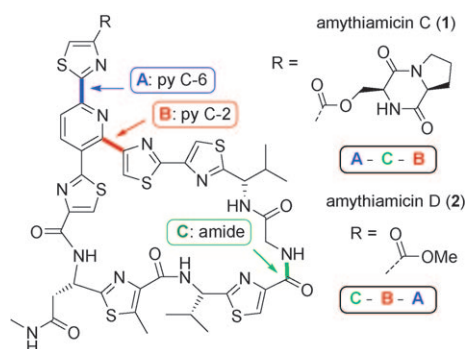
Spiroacetal out of control! A unique and practical synthetic sequence to allow rapid access to polyketides and further to the spiroacetals derived from them is reported (see scheme).

The synthesis utilizes a bidirectional Hosomi–Sakurai allylation approach around key allylsilanes in the synthesis of the AB and CD ring systems of spongistatin 1 and 2.

Spiro Compounds

C. L. Flowers, P. Vogel* . 14074–14082

Short Diastereoselective Synthesis of the C1–C13 (AB Spiroacetal) and C17–C28 Fragments (CD Spiroacetal) of Spongistatin 1 and 2 through Double Chain-Elongation Reactions



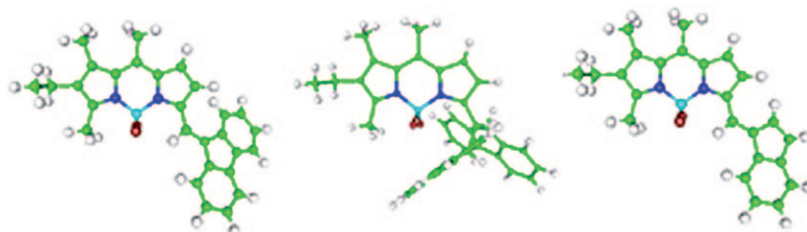
Cross-coupling reactions paved the way to two short syntheses of amythiamicin C (**1**) and D (**2**; see scheme). In the former synthesis, the sequence A–C–B was followed to give access to the

title compound **1**. In the latter synthesis, the sequence C–B–A was probed and led successfully to amythiamicin D (**2**) in an extremely short, but less selective, synthetic sequence.

Natural Products

C. Ammer, T. Bach* 14083–14093

Total Syntheses of the Thiopeptides Amythiamicin C and D



It's all under control: A strategy to modulate the photophysical and optical properties of BODIPYs by using asymmetric substitution effects has

been developed. New asymmetric BODIPY–indene and BODIPY–fluorene dyes have been synthesized (see figure) by a simple protocol.

Fluorescent Molecules

J. Bañuelos-Prieto,* A. R. Agarrabeitia, I. Garcia-Moreno, I. Lopez-Arbeloa, A. Costela, L. Infantes, M. E. Perez-Ojeda, M. Palacios-Cuesta, M. J. Ortiz* 14094–14105

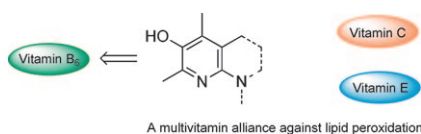
Controlling Optical Properties and Function of BODIPY by Using Asymmetric Substitution Effects



Antioxidants

R. Serwa, T.-g. Nam, L. Valgimigli,
S. Culbertson, C. L. Rector,
B.-S. Jeong,* D. A. Pratt,*
N. A. Porter 14106–14114

Preparation and Investigation of Vitamin B₆-Derived Aminopyridinol Antioxidants



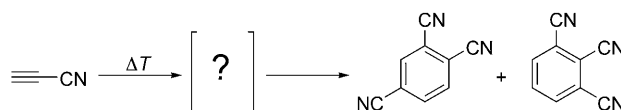
Oxidatively stressed? Take a vitamin!

An efficient and highly practical synthetic route for pyridinol-based antioxidants from vitamin B₆ is reported. Antioxidant properties for new members of this family of radical scavengers have been investigated. It was discovered that these amino-pyridinols are able to not only inhibit lipid peroxidation in direct reaction with peroxy-radicals but also act as co-antioxidants in the presence of vitamin E as previously reported for vitamin C (see scheme).

Cyanoacetylene

H. Hopf,* C. Mlynek, R. J. McMahon,*
J. L. Menke, A. Lesarri, M. Rosemeyer,
J.-U. Grabow* 14115–14123

On the Trimerization of Cyanoacetylene: Mechanism of Formation of Tricyanobenzene Isomers and Laboratory Detection of Their Radio Spectra



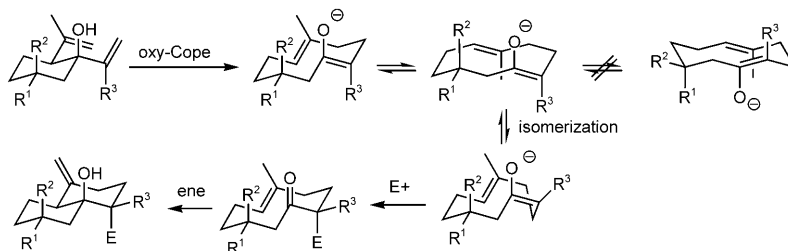
The final frontier: To better understand the chemistry of cyanoacetylene—a known constituent of planetary atmospheres and interstellar space—theoretical and spectroscopic studies

address the mechanism of its di- and trimerization, and provide high-resolution rotational spectra of two of the trimers: 1,2,3- and 1,2,4-tricyanobenzene (see picture).

Cope Reaction

J. Hooper, E. L. O. Sauer, S. Arns,
T. K. Woo,*
L. Barriault* 14124–14130

On the Origin of Altered Diastereomeric Ratios for Anionic versus Neutral Reaction Conditions in the Oxy-Cope/Ene Reaction: An Interplay of Experiment and Computational Modeling



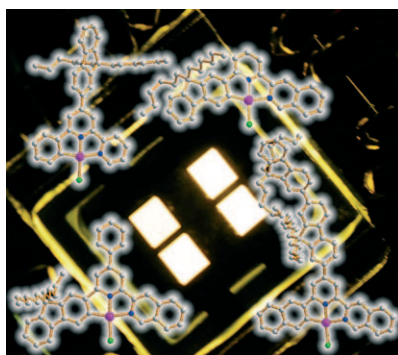
Carbanions at play: A sequential oxy-Cope/ene reaction, engineered to produce decalin skeleton structures for further applications in natural product synthesis, was found to give altered product distributions under anionic

conditions. With DFT calculations and ab initio molecular dynamics simulations, its altered diastereoselectivity is shown to be the result of a hitherto unexpected isomerization of the enolate olefin (see scheme).

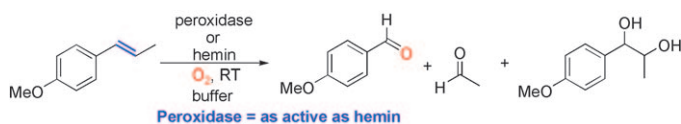
Organic Light-Emitting Diodes

M.-Y. Yuen, S. C. F. Kui, K.-H. Low,
C.-C. Kwok, S. S.-Y. Chui, C.-W. Ma,
N. Zhu, C.-M. Che* 14131–14141

Synthesis, Photophysical and Electrophosphorescent Properties of Fluorene-Based Platinum(II) Complexes



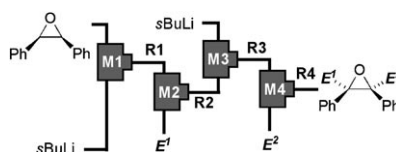
Molecularly doped PLEDs, based on poly(9-vinylcarbazole) (PVK) blended with phosphorescent fluorene-substituted cyclometalated platinum(II) complexes as dopants (see figure), exhibit excellent performance and good efficiency. A polymer light-emitting diode (PLED) containing 5% fluorene-based platinum(II) complex shows a high current efficiency of 9.2 cd A⁻¹ with a brightness of 3500 cd m⁻².



Go catalytic! It has been shown that peroxidases are able to cleave selected C=C double bonds adjacent to activated phenyl moieties at the expense of molecular oxygen at an acidic pH as

a promiscuous activity (see scheme). We could unambiguously prove that exclusively the hemin moiety present in the enzyme is responsible for this activity.

Flow microreactor system: An integrated flow microreactor system serves as a powerful method for the stereoselective synthesis of substituted epoxides (see figure).



Enzyme Catalysis

*F. G. Mutti, M. Lara, M. Kroutil, W. Kroutil** 14142–14148

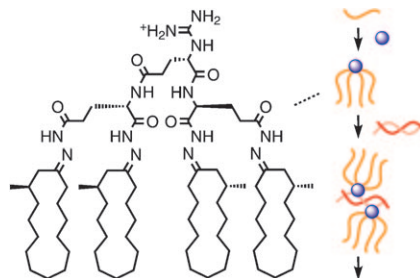
Ostensible Enzyme Promiscuity: Alkene Cleavage by Peroxidases

Epoxidation

*A. Nagaki, E. Takizawa, J.-i. Yoshida** 14149–14158

Generation and Reactions of Oxiranyl-lithiums by Use of a Flow Microreactor System

Fragrant multitail amphiphiles: The in situ product of hydrophobic odorant analytes, such as muscone (see figure), and cationic multihydrazide peptide dendrons are introduced as powerful activators of DNA transporters for application indifferent sensing, cellular uptake, slow release, and fluorescent labeling.

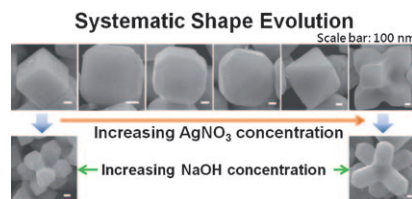


Supramolecular Systems

*J. Montenegro, P. Bonvin, T. Takeuchi, S. Matile** 14159–14166

Dynamic Octopus Amphiphiles as Powerful Activators of DNA Transporters: Differential Fragrance Sensing and Beyond

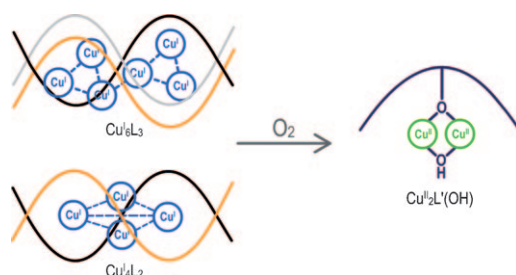
Shaping the future: Ag_2O crystals with shapes from cubic to edge- and corner-truncated cubic, rhombicuboctahedral, edge- and corner-truncated octahedral, octahedral, and hexapod structures have been synthesized. By adjusting the reaction conditions, octapods and elongated hexapods can be prepared. Octahedra and hexapods with {111} facets are sensitive to the molecular charges in the solution.



Nanostructures

*L.-M. Lyu, W.-C. Wang, M. H. Huang** 14167–14174

Synthesis of Ag_2O Nanocrystals with Systematic Shape Evolution from Cubic to Hexapod Structures and Their Surface Properties



Capable presence: Copper(I) cluster helicates derived from a thiosemicarbazone ligand can hydroxylate the arene linker of their supporting ligand

strands in the presence of O_2 . The kinetic studies show values of $\Delta H^\ddagger = -70 \text{ kJ mol}^{-1}$, similar to those mediated by the tyrosinase enzymes.

Supramolecular Chemistry

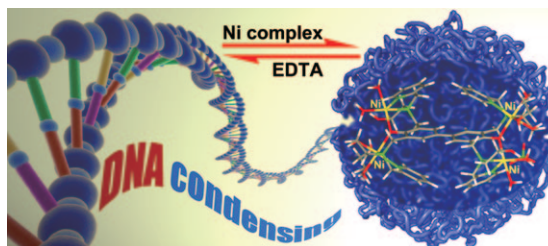
M. Martínez-Calvo, M. Vázquez López, R. Pedrido, A. M. González-Noya, M. R. Bermejo, E. Monzani, L. Casella,* L. Sorace* . . . 14175–14180

Endogenous Arene Hydroxylation Promoted by Copper(I) Cluster Helicates

DNA Condensation

X. Dong, X. Wang,* Y. He, Z. Yu,
M. Lin, C. Zhang, J. Wang, Y. Song,
Y. Zhang, Z. Liu, Y. Li,
Z. Guo* 14181–14189

Reversible DNA Condensation Induced by a Tetranuclear Nickel(II) Complex



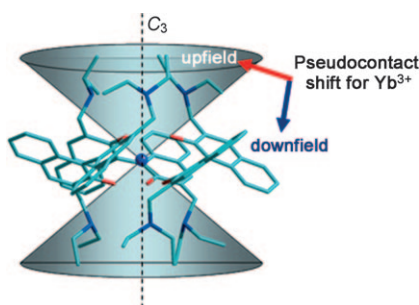
Nonviral vector: A tetranuclear nickel(II) complex has been designed and prepared as a nonviral vector for gene therapy. The complex can induce the condensation of DNA into nanoparticles through electrostatic interactions. The release of DNA from the compact

state has been realized using the chelator ethylenediaminetetraacetic acid (EDTA) for the first time (see graphic). Along with biocompatibility and nuclease-inactivity, the complex meets most of the prerequisites for a gene vector.

Lanthanide Complexes

L. Di Bari,* S. Di Pietro, G. Pescitelli,
F. Tur, J. Mansilla,
J. M. Saá* 14190–14201

[Ln(binolam)₃](OTf)₃, a New Class of Propeller-Shaped Lanthanide(III) Salt Complexes as Enantioselective Catal- ysts: Structure, Dynamics and Mecha- nistic Insight



A class of their own: The solution structure (see picture) and dynamics of lanthanide–binaphthol amine compounds bearing Lewis acid, Brønsted acid and Brønsted base groups are determined with paramagnetic NMR spectroscopy and circular dichroism. The complexes are active as enantioselective catalysts in the nitroaldol reaction.

* Author to whom correspondence should be addressed

Supporting information on the WWW (see article for access details).

VIP Full Papers labeled with this symbol have been judged by two referees as being “very important papers”.

Video A video clip is available as Supporting Information on the WWW (see article for access details).

SERVICE

Spotlights 13906 Author Index 14204 Keyword Index 14205 Preview 14207

Issue 46/2010 was published online on December 3, 2010



Fast, Individual, Popular...
REPRINTS
Available to order anytime!
Contact Carmen Leitner (e-mail: chem-reprints@wiley.com)